analytical chemistry

Article

pubs.acs.org/ac

Electrophoretic Migration and Particle Collisions in Scanning Electrochemical Microscopy

Aliaksei Boika† and Allen J. Bard*

Center for Electrochemistry, Department of Chemistry and Biochemistry, University of Texas at Austin, 105 East 24th Street Station A5300, Austin, Texas 78712, United States

Supporting Information

ABSTRACT: We report for the first time how electrophoretic migration of ions and charged nanoparticles (NPs) in low electrolyte concentration solutions affects positive feedback in scanning electrochemical microscopy (SECM). The strength of the electric field in the gap between either the tip and the substrate, or the tip and counter electrodes, is shown to increase proportionally to the decrease in gap size. This field affects the flux of the charged redox species as expected for dilute electrolyte solutions. However, the shape of the normalized approach curve is unaffected by the electrophoretic migration. We also report that the rate of collisions of charged insulating NPs with the tip electrode decreases as the tip is brought closer to the substrate electrode. This rather unexpected result (negative feedback) can be explained by the blocking of the particle flux with the glass insulating layer around the metal microwires. Observation of simultaneous changes in the faradaic current at the tip and substrate electrodes due to particle collisions with the tip confirms a high rate of mass transport between the two electrodes under the conditions of positive feedback SECM.

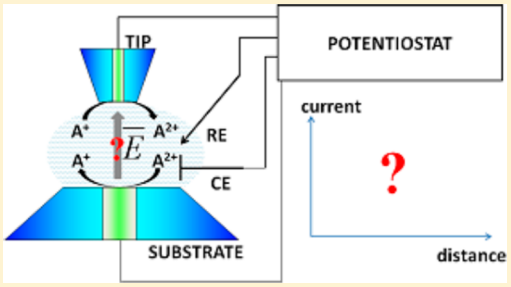

Scanning electrochemical microscopy (SECM) is a well-established and powerful technique that is used extensively in fundamental studies and analytical applications.[1] However, to date, all theoretical treatments of SECM experiments have assumed that the mass transport of redox species occurs exclusively by diffusion. In this paper, we investigate how SECM measurements are affected by electrophoretic migration under conditions of low concentrations of supporting electrolyte. Our findings are important for fundamental research and have significant implications in the area of electroanalytsis.

Such considerations are especially interesting in the area of single molecule detection. For example, Fan and Bard have shown that individual redox molecules can be detected in the gap between two electrodes by way of their repetitive cycling and transfer of charge (i.e., amplification).[2] If a molecule in the gap moves only by diffusion, then the amplification factor (number of cycles between the electrodes in a second) can reach 10^7, and the measured faradaic current is on the order of 1 pA. However, one can envision the possibility that if an additional mode of mass transfer is introduced into the system (i.e., migration of the charged species (molecules or nanoparticles, NPs) due to performing the experiments under low electrolyte solutions), then the amplification factor of the species could increase even more, leading to an improved sensitivity of their electrochemical detection. In a recent study, we have shown that electrophoretic migration can be a dominant mode of mass transfer of charged NPs.[3] The flux of nanoparticles, driven by migration, scales proportionally to the flux of the redox species (i.e., the faradaic current (the effect of nanoparticle flux on the faradaic current is negligible)). Thus, because under positive feedback conditions in SECM the flux of depolarizer in the interelectrode gap can increase by a factor of 10 and higher, the frequency of NP collisions could increase by the same factor. If true, this finding could then assist in the analysis of very low concentrations of analyte species, subfemtomolar and less.

Methods of stochastic electrochemical detection offer exceptional sensitivity to the detection of a number of analyte species, including metal NPs (Pt,[4] Au,[5] Ag[6−8]), insulating beads (i.e., polystyrene and silica),[3] carbon nanotubes,[9] organic particles[10] and emulsions.[11] Although the variety of available detection approaches (direct electrolysis, electrocatalytic amplification,[12] electrode area blocking and increase, and change in the open-circuit potential[13]) indicates that new systems for analysis will be found in the course of future research, an effort is also being made to understand the mass transport of the analytes to the electrode. Knowledge of the exact relationship between the concentration of the analytes and the frequency of the observed collision events constitutes the cornerstone of analytical methodologies being developed. The simplest detection schemes are based on the transfer of analyte species to the sensor by diffusion; this allows determination of analytes in the picomolar to tens of picomolar concentration range. Significantly lower detection limits (low femtomolar concentrations) can be reached by using electrophoretic migration of the analytes in order to bring them to the electrode for subsequent detection.[3] Thus, investigation of the

Received: July 25, 2014
Accepted: November 4, 2014
Published: November 4, 2014

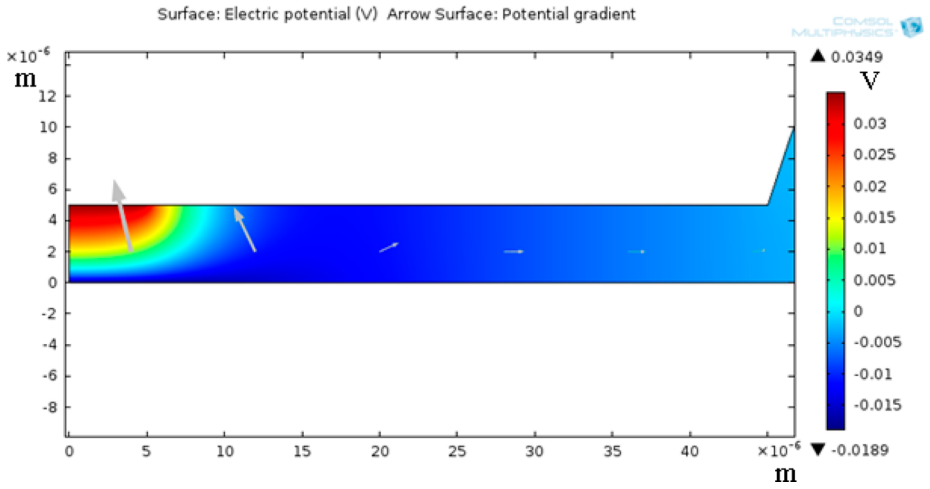

Figure 1. Electric potential distribution in solution with low supporting electrolyte concentration (0.1 mM 1:1 electrolyte) in a gap between the tip and substrate electrodes (four-electrode configuration). Tip radius, 5 μm (RG = 9), substrate radius, 25 μm; tip-to-substrate separation, 5 μm. Concentration of the redox species (FcMeOH), 3 mM. Tip is biased at a potential of mass transfer controlled oxidation of FcMeOH, substrate is held at the potential of mass transfer controlled reduction of $FcMeOH^+$. Gray arrows indicate the direction of the electric potential gradient.

effect of electrophoretic migration on mass transfer of charged molecules and particles under the conditions of SECM experiments has the potential to advance the field of single molecule and particle detection significantly.

To the best of our knowledge, there are no reports describing the effect of electrophoretic migration on mass transport of charged species under the conditions of SECM experiments. Mirkin et al. investigated the effect of ionic strength on the shape of cyclic voltammograms obtained under the condition of a nanometer-sized thin-layer cell.[14] The nature of the observed effects under their conditions has been explained by the electrophoretic migration of the charged species and the double-layer effects on the nanoscale. The presented work is different in that we propose a theoretical model of migration phenomena and our primary interest is to investigate the mass transfer of ions and colloidal particles under the migration SECM conditions. In terms of stochastic electrochemical detection in the SECM arrangement, the first example was given by Kwon and Bard, who studied IrO_x nanoparticle (NP) collisions and investigated the nature of the NP interaction with the electrode.[15] By using the diffusion-controlled NP mass transfer model, it has been shown that IrO_x NPs, upon collision with the electrode surface, are deactivated due to electrochemical production of oxygen at the particle surface in the course of the oxygen evolution reaction.

The results presented in this paper include both theoretical and experimental findings on the effect of migration on mass transport of charged species in the gap between the tip and substrate electrodes. It is shown that by decreasing the size of the gap in an SECM experiment in solution with low supporting electrolyte concentration the strength of the electric field increases proportionally. However, the shape of the normalized approach curve is unaffected by migration (i.e., it is the same as for the diffusion-controlled mass transfer process independent of electrolyte concentration and mediator charges). Even when the strength of the electric field increases as the gap is made smaller, the frequency of NP collisions decreases; this negative feedback effect is rationalized in terms of the blockage of the flux of the particles to the tip by the insulating glass sheath around the electrodes.

EXPERIMENTAL SECTION

Materials and Instrumentation. All chemicals used to prepare solutions were ACS grade and were not purified additionally before the experiments. The spherical particles used in collision experiments were unfunctionalized polystyrene (1 μm diameter) and were purchased from Bangs Laboratories, Inc. (Fishers, IN; catalog number PS04N). These spheres were supplied in aqueous solutions containing sodium dodecyl sulfate and sodium azide. To remove the unwanted chemicals, the spheres were washed by centrifugation with water before experiments. All solutions were prepared using water from Millipore reagent grade purification system (Millipore, Bedford, MA). Ferrocenemethanol was purchased from Alfa Aesar (Ward Hill, MA), potassium nitrate, from Fisher Scientific (Hampton, NH).

Microelectrodes were constructed by sealing metal microwires (Pt or Au) in borosilicate glass. To achieve the required RG factor of the tip (RG = r_d/r_{tot}, where r_d is the radius of the microwire used to make a disk microelectrode and r_{tot} is the total radius of the tip including the glass insulation), the glass sheath was polished manually using sandpaper until the required shape was achieved.

Electrochemical measurements were performed using a CH Instruments scanning electrochemical microscope, model CHI920c. The electrochemical cell was custom-made from Teflon and had either a three-electrode or four-electrode configuration (fourth electrode being the second working electrode). All experiments were done without the removal of dissolved oxygen.

SECM Measurements. To create a gap of a known size between two electrodes (the tip and substrate, or the tip and counter electrode), the tip is brought to the other electrode by moving translation stages of the SECM while simultaneously monitoring the faradaic current. The exact position of the tip is then determined from the value of the limiting current recorded under the conditions of purely diffusional mass transfer of the redox species (i.e., high concentration of the supporting electrolyte). In Scheme S1 (Supporting Information), one can see the actual gap created in the manner described. Note that the movement of the tip electrode can be done using either the stepper or piezo motors. However, to minimize the effect of

dx.doi.org/10.1021/ac502944n | Anal. Chem. 2014, 86, 11666−11672

hysteresis on current measurements, the movement of the tip in the vicinity to the substrate was done with the piezo stage only.

Numerical Simulations. Simulations discussed in this paper were done using the model developed in COMSOL Multiphysics software (COMSOL, Sweden). All relevant equations, including the boundary and initial conditions, are described in the Supporting Information. In short, the model solves the Nernst–Plank equation assuming the electroneutrality condition.

RESULTS AND DISCUSSION

Theoretical Considerations. We begin by considering the theoretical models for the SECM experiments under the condition of low concentration of electrolyte in solution. In this regard the following two cases can be considered: 1) approach of a tip electrode to a conductive substrate electrode with a counter and reference electrodes positioned in the bulk solution (four-electrode configuration, the substrate is biased), and 2) approach of the tip to the counter electrode also acting as the substrate electrode (reference electrode in the bulk). Both cases fulfill the positive feedback condition in the SECM experiment: the product of the redox process at the tip electrode is recycled at the surface of the substrate, whether it is a counter electrode surface or not. As a result, the flux of the redox species at the tip increases (as well as the faradaic current density) proportional to the separation distance between the tip and substrate electrodes. Thus, an interest in the theoretical simulations is to see how the electric field, which is responsible for migration, is affected by the parameters of the experiment (i.e., the size of the gap and the dimensions of the electrodes).

In our previous paper, we have considered the effect of the electrode radius and the concentrations of the redox species and the supporting electrolyte ions on the strength of the electric field leading to migration.[3] Similar to this, if the tip electrode is far away from the substrate ($L \geq 30$, where $L = d/a$ with d being the separation between electrodes and a, the radius of the tip), its behavior is essentially the same as discussed before: the electric field strength scales with the magnitude of the faradaic current density and is affected by the concentrations of the redox species and the supporting electrolyte, and the radius of the electrode. However, if the tip is brought closer to the substrate (Figure 1, four-electrode configuration with the substrate electrode biased), the flux of the redox species to the tip increases due to the aforementioned recycling of the species at the substrate. Thus, the faradaic current at the tip and the substrate electrodes (positive feedback, not shown), as well as the electric potential gradient in the gap in between the two, increase as shown in Figure 2 for the electric potential.

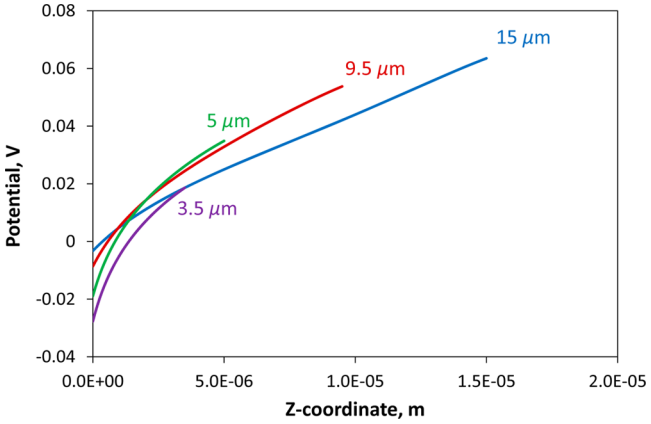

Figure 2. Electric potential distribution in solution with low supporting electrolyte concentration (0.1 mM) along a line going through the centers of the tip and substrate electrodes (z-coordinate). $z = 0$ corresponds to the surface of the substrate electrode, whereas z = 3.5, 5, 9.5, or 15 μm corresponds to the surface of the tip. Tip radius, 5 μm (RG = 9), substrate radius, 25 μm; tip-to-substrate separation between 3.5 and 15 μm (indicated beside each curve). Concentration of the redox species (FcMeOH), 3 mM. Tip is biased at a potential of mass transfer controlled oxidation of FcMeOH, substrate is held at the potential of mass transfer controlled reduction of $FcMeOH^+$ (four-electrode configuration) Approximate electric field strengths (assuming linear potential profiles): 4.45 kV/m (15 μm), 6.57 kV/m (9.5 μm), 10.8 kV/m (5 μm), 13.2 kV/m (3.5 μm).

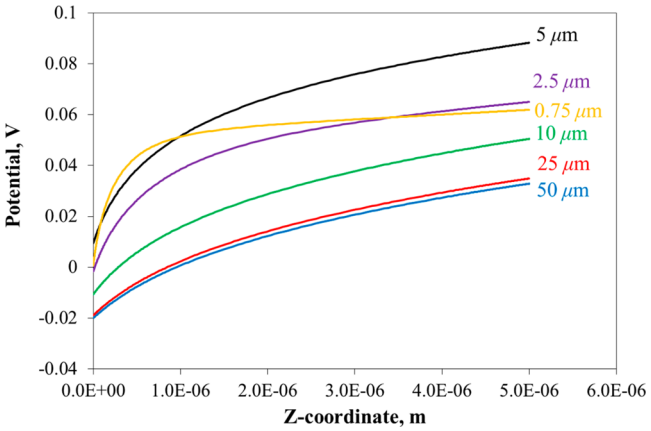

Figure 3. Electric potential distribution in solution with low supporting electrolyte concentration (0.1 mM) along a line going through the centers of the tip and substrate electrodes (z-coordinate). $z = 0$ corresponds to the surface of the substrate electrode, whereas z = 5 μm corresponds to the surface of the tip. Tip radius, 5 μm (RG = 9), substrate radius, between 0.75 and 50 μm (indicated beside each curve). Concentration of the redox species (FcMeOH), 3 mM. Tip is biased at a potential of mass transfer controlled oxidation of FcMeOH, substrate is held at the potential of mass transfer controlled reduction of $FcMeOH^+$. Approximate electric field strengths (assuming linear potential profiles): 10.6 kV/m (50 μm), 10.8 kV/m (25 μm), 12.2 kV/m (10 μm), 15.8 kV/m (5 μm), 13.3 kV/m (2.5 μm), 12.2 (0.75 μm).

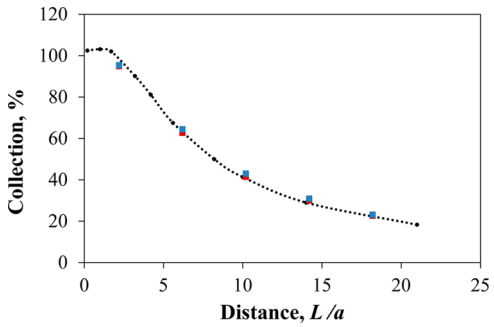

Figure 4. Collection efficiency of $FcMeOH^+$ on a substrate electrode as a function of the tip-to-substrate separation and the supporting electrolyte concentration. Tip, 5 μm radius Au disk (RG = 9); substrate, 25 μm radius Au disk. Concentration of FcMeOH was 3 mM, while the supporting electrolyte concentration was 0 mM KNO_3 (red squares) and 100 mM KNO_3 (blue squares). The dotted line corresponds to the simulated data obtained using the COMSOL model.

dx.doi.org/10.1021/ac502944n | Anal. Chem. 2014, 86, 11666–11672

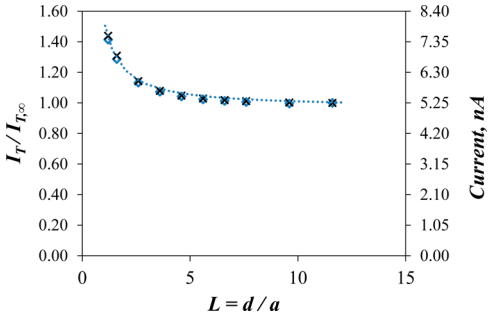

Figure 5. Dimensionless approach curves to a platinum counter electrode (1 mm diameter, 2 mm length) recorded in 3 mM FcMeOH, 0.4 mM KNO_3 (◊) and 40 mM KNO_3 (×). Tip electrode used in the experiment was 5 μm radius Au disk (RG = 9). Dotted line represents an analytical solution for an approach curve to a conductive substrate under diffusion-controlled positive feedback conditions.

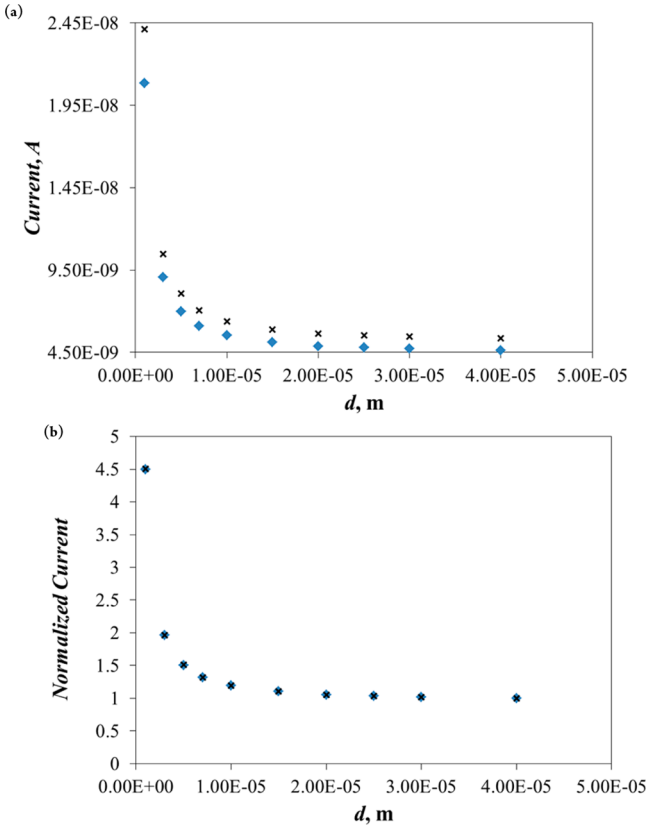

Figure 6. (a) Simulated approach curves for the oxidation of 3 mM A^+ to A^{2+} species at a 5 μm radius tip (RG = 9) in 0.4 mM (blue diamonds) and 400 mM (black crosses) 1:1 electrolyte. The tip was positioned over a counter electrode 1 mm in diameter; d is the distance between the electrodes. (b) Normalized approach curves for the data in panel a.

The electric potential profiles in Figure 2 represent the values of the potential along a line going through the centers of the tip and substrate electrodes. These profiles are not linear, which can be explained by the geometry of the gap: the mass transfer of the species can occur along the axis going through the centers of the electrodes, and also radially, in the direction parallel to the surface of the tip and the substrate. As the size of the gap decreases, the magnitude of the electric field between the tip and substrate electrodes increases; this is evidenced by the increase in the slope of the potential profile curves in Figure

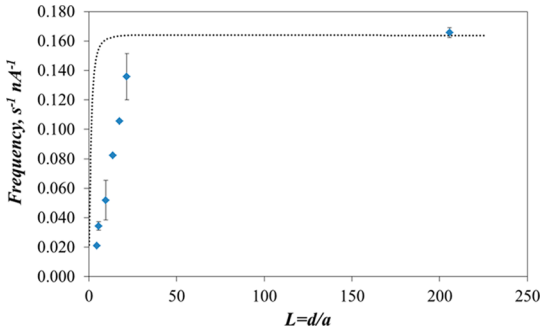

Figure 7. Normalized collision frequency (frequency (in s^{-1})/average current (in nA)) of polystyrene particles (1 μm in diameter) with the surface of a 5 μm radius Au tip disk (RG = 9) positioned above a 25 μm radius Au substrate disk microelectrode, as a function of the tip-to-substrate separation L; d is the distance between the tip and the substrate, and a is the radius of the tip electrode. Concentration of the redox species (FcMeOH), 4 mM. Particle concentration, 87 fM. Tip was biased at a potential (+0.1 V) corresponding to the steady-state oxidation of FcMeOH, substrate was biased at a potential (−0.4 V) corresponding to the mass transfer limited reduction of $FcMeOH^+$ produced at the tip. Reference electrode was mercury/mercurous sulfate in saturated potassium sulfate solution. Dotted line represents change in the normalized current at the tip due to negative feedback in SECM; it was calculated using an analytical expression for RG = 10 tip found in reference 1 and included in the Supporting Information.

2. Thus, by bringing the tip and the substrate closer to each other in the low electrolyte concentration medium, the strength of the electric field and the magnitude of migration effect in the interelectrode gap increase. Similar findings were also established for the case of the tip approach to the counter electrode surface, as shown in Figures S1 and S2 in the Supporting Information.

In Figure 3, one can see the effect of the substrate electrode size on the magnitude of the electric potential in the gap. When the size of the substrate is much bigger than that of the tip, the field between the electrodes is essentially the same. This can be explained by essentially the same faradaic current density in the gap. However, once the size of the substrate is made more comparable to the tip electrode, the potential gradient increases. Finally, once the substrate is substantially smaller than the tip, the electric field is the most nonlinear: closer to the substrate, along the center symmetry axis, it is much stronger than further to the tip. Similarly to the data in Figure 2, these results can be explained by the complex nature of the mass transfer of the species in the gap and the fact that the current density in the interelectrode gap increases as the substrate electrode is made comparable in size to the tip.

As shown by the data in Figures 1, 2, S1 and S2 (Supporting Information), both cases of the tip approach to the substrate and counter electrodes give qualitatively similar results. The difference is only in that, for the approach to the substrate electrode, there is a component of the current flowing to the counter electrode and thus escaping the gap. As a result, the electric field in the interelectrode gap is somewhat smaller than for the case of the approach to the counter electrode. However, the effect is relatively small because the magnitude of the electric field decreases very quickly away from the tip and substrate/counter electrodes (gray arrows in Figures 1 and S1 (Supporting Information)).

It should be noted that the flow of the faradaic current and the electric field in solutions with a low supporting electrolyte

dx.doi.org/10.1021/ac502944n | Anal. Chem. 2014, 86, 11666−11672

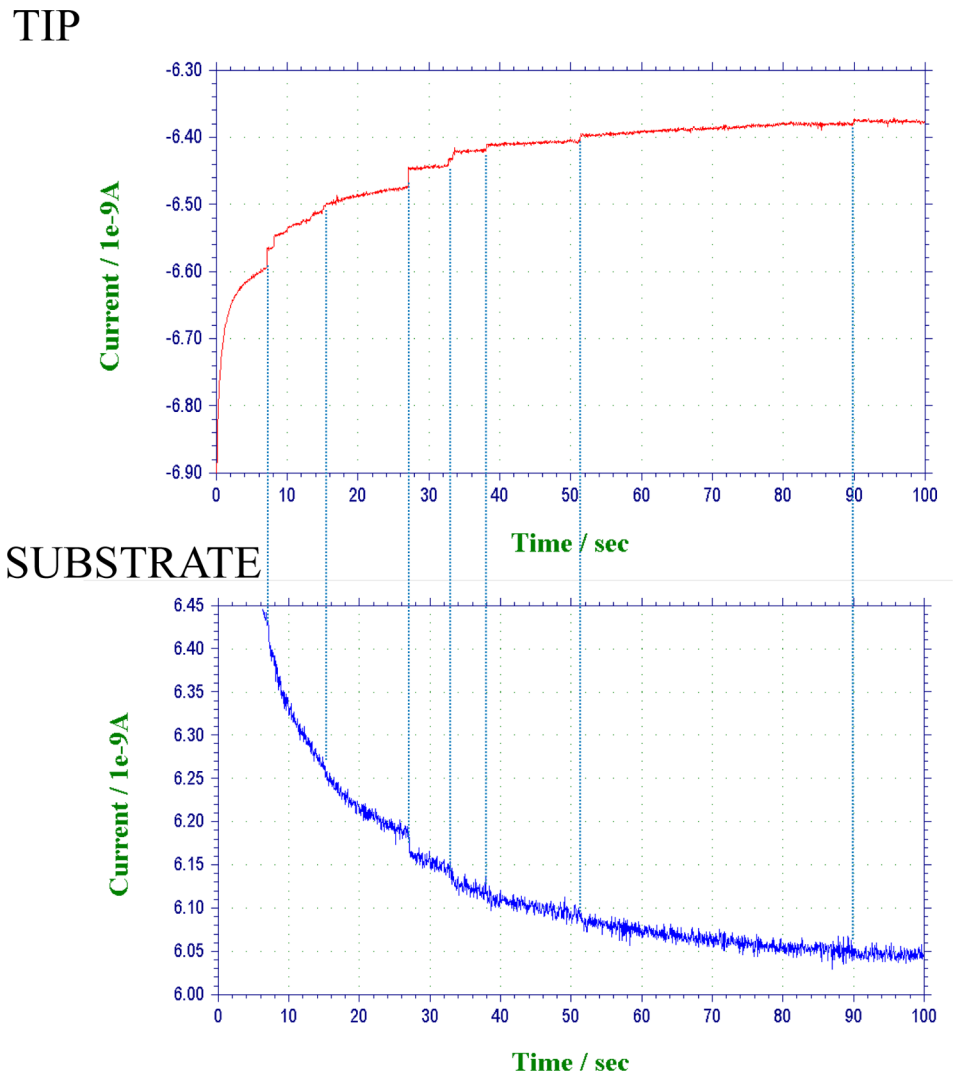

Figure 8. Chronoamperograms recorded with a tip (5 μm radius Au disk, RG = 9) and substrate (25 μm radius Au disk) electrodes separated by a distance of 5 μm in solution containing 4 mM FcMeOH. Potential applied to the tip was +0.1 V and corresponded to the mass transfer limited oxidation of FcMeOH. Potential applied to the substrate was −0.4 V and corresponded to the mass transfer limited reduction of $FcMeOH^+$ produced at the tip. The solution also contained 87 fM polystyrene beads 1 μm in diameter. Reference electrode was mercury/mercurous sulfate in saturated potassium sulfate solution. Dotted blue lines correlate simultaneous changes in faradaic currents observed at the tip and substrate electrodes due to the particle collisions with the tip electrode surface.

concentration are interconnected. In a four-electrode configuration (counter and reference electrodes are in the bulk solution) under the conditions of positive feedback, the redox mediator is recycled in a gap between the tip and substrate electrodes. As a result, the faradaic current density is the highest in the gap. However, depending on the separation between the tip and the substrate, some of the redox mediator species are able to escape from the gap (i.e., there is a non-negligible current flow between the tip and the counter electrodes). In solutions with no supporting electrolyte or with a low electrolyte concentration, this transliterates to the presence of the component of the electric field directed away from the gap and toward the counter electrode (indicated by the gray arrows pointing to the right in Figure 1). As a result, the sign of the electric potential appears to be changing when moving toward the edge of the tip.

Experimental Approach Curves and Generation–Collection Experiments. To further test the presence of migration effect in SECM experiments, we have conducted two sets of experiments. In the first set of experiments (Figure 4), we investigated how the collection efficiency of hydroxymethylferrocenium ions (the product of the reaction at the tip) depends on the concentration of the supporting electrolyte in solution and the size of the gap. The idea behind these experiments was that due to the electric field present in the gap between the tip and substrate electrodes in low electrolyte concentration solution, the collection efficiency of $FcMeOH^+$ should vary depending on the gap size and the electrolyte concentration. This was a plausible expectation because the results in Figures 1, 2, S1 and S2 (Supporting Information) clearly show the presence of the electric field, the strength of which increases as the gap is made smaller. However, no effect of the electrolyte concentration had been observed; the collection efficiency of $FcMeOH^+$ was the same both in low and high electrolyte concentration solutions at the same separation between the tip and substrate electrodes. In addition, the results of the experiments agreed well with the simulated

dx.doi.org/10.1021/ac502944n | Anal. Chem. 2014, 86, 11666−11672

values of the collection efficiency of $FcMeOH^+$ given by the black dotted curve in Figure 4.

In the second set (Figure 5), two approach curves to a counter electrode were recorded: the first one in a high electrolyte concentration solution (40 mM KNO_3) and the second in the low electrolyte concentration solution (0.4 mM KNO_3). In both cases, the concentration of the redox species, ferrocenemethanol (FcMeOH), was 3 mM and all other experimental conditions were the same. The potential applied to the tip electrode corresponded to the mass transfer controlled oxidation of FcMeOH, and the positive feedback was observed once the tip was brought close to the counter electrode in both cases. An interesting finding was that the approach curves were identical, which suggests that under the experimental conditions in Figure 5, migration does not affect the shape of the curves.

The experimental findings presented in Figures 4 and 5 do not indicate the absence of the electric field in the electrode gap, but merely that this field does not affect the normalized or dimensionless mass transfer of the redox species under the conditions of the experiments. Due to steady-state oxidation of FcMeOH at the tip electrode, its flux to the substrate has to be equal to the flux of $FcMeOH^+$ back to the tip. Thus, because FcMeOH is uncharged, its mass transfer rate is not affected by the electric field present in the gap, and the overall result of the corresponding experiments looks as if no migration effect exists. But, in fact, the electric field is present in the gap between the tip and substrate electrodes in low electrolyte concentration solutions, as suggested by the results of the simulations in Figures 1−3 and S1 and S2 (Supporting Information).

If both the reactant and the product of the reaction at the tip electrode are charged, then we expect to see the change in the absolute value of the faradaic current due to the migration effect in solutions with low supporting electrolyte concentrations. This is supported by the results of the simulations shown in Figure 6a. However, if the tip current is normalized with respect to its value in the bulk solution, the normalized approach curve looks the same as in the case of purely diffusional mass transfer of the redox species, Figure 6b. The "elimination" of the migration effect by normalization of faradaic currents can be explained intuitively by the fact that the fluxes of species in the interelectrode gap are interconnected. The decrease in the flux of the positively charged redox species at the tip due to the presence of the electric field means that, in steady state, the rate of the product "recycling" at the substrate electrode also decreases proportionally. As a result, the normalized approach curve stays the same as for the case of purely diffusional mass transport of redox species. Similar findings were also observed for +2/+3 redox couple in the interelectrode gap, and also with no supporting electrolyte present in solution.

Charged Particle Collisions in the Interelectrode Gap. We now consider the effect of the electric field in the gap on behavior of charged particles. Simple theoretical considerations indicate that the mass transport of charged particles should be affected by the electric field in the electrode gap much more than in case of ions, since the particles are bigger and carry much larger charge. Equation 1 allows estimation of the time it takes a charged particle or ion to traverse a distance d in the electric field. The derivation of this equation is included in the Supporting Information (eqs S5−S7).

$$\frac{t_m}{t_d} = \frac{2d}{|z|(F/RT)E} \quad (1)$$

where t_m is the travel time by migration, t_d is the travel time by diffusion, z is the charge, E is the strength of the electric field and the other symbols have their usual meanings.

Thus, for all other parameters in eq 1 being the same, the time of travel of an ion or a particle by migration is inversely proportional to its charge, z. As a result, for simple ions such as hydroxymethylferrocenium cation ($z = 1$), the time of travel by migration and diffusion are similar considering the magnitude of the electric field (Figures 1 and 2). However, larger colloid particles that carry a bigger charge (silica, citrate capped Pt NPs, polystyrene beads) should be traveling by migration proportionally faster. According to our experience,[3] the absolute value of the charge (directly related to the ζ-potential) of 1 μm polystyrene beads can reach over −10 000; thus, very high rates of their migrational transfer are possible.

To investigate the effect of the electric field in the interelectrode gap on mass transport of charged particles, the frequency of NP collisions with the tip electrode was determined experimentally as a function of the tip-to-substrate separation. Blocking collisions of polystyrene beads (1 μm in diameter) with the tip electrode (5 μm radius Au disk) were monitored at each separation distance for 100 s (so the frequency was determined as the number of collisions divided by 100 s); the results are presented in Figure 7. Further experimental conditions are listed in the Supporting Information

Here the normalized frequency of collisions (expressed as the number of collisions in 100 s divided by the average faradaic current during the observation period) is plotted as a function of the distance between the tip and substrate electrodes. When the separation between the electrodes is very large (the rightmost point in Figure 7), the rate of NP collisions is independent of the presence of the substrate electrode. However, as the tip is brought closer to the substrate, a negative feedback is observed. This was a rather surprising result because an increase in the frequency of collisions was expected due to an increase in the strength of the electric field in the gap at short separation distances (Figure 2). An explanation to these data comes from realizing that upon approach of the substrate with the tip, fewer particles are left in the gap between the electrodes because the average interparticle distance is rather large. For the concentration of the particles used in the experiment, this distance is estimated to be about 3 μm. So, when the gap is small, the number of particles in the vicinity of the electrodes (and the strongest electric field area) decreases. As a result, a negative feedback for the collision frequency is observed even though the strength of the electric field increased according to the data in Figure 2.

Observation of nanoparticle collisions when the gap between the tip and substrate electrodes is small provides strong evidence for a high rate of mass transport of the redox species between the electrodes under the positive feedback conditions. In Figure 8, one can see that when the interelectrode separation is only 5 μm, the change in the tip current due to insulating particle collisions with the tip surface is accompanied by essentially simultaneous changes in the faradaic current at the substrate electrode, even though no NP collisions are expected to occur with the substrate under the conditions of the experiment. The substrate response arises only because of the transient change in the tip current that is transmitted via the feedback to the substrate. These data also support the findings in Figures 1 and 2, suggesting that upon approach of the tip and substrate electrodes to distances comparable to the size of these

dx.doi.org/10.1021/ac502944n | Anal. Chem. 2014, 86, 11666−11672

electrodes, the flux of the redox species in the gap and the electric field increase proportionally. Note that at higher separations between the tip and substrate electrodes, no changes in the substrate current were observed when the particle collisions occurred at the tip. Once again, this supports the idea that the flux of the redox species (positive feedback) and the strength of the electric field in solutions with low electrolyte concentrations are substantial only at small interelectrode gaps.

Our findings presented above indicate that by bringing the tip electrode to the substrate to distances comparable to the size of these electrodes, one can increase the strength of the electric field responsible for the migration effect. This is supported by theoretical simulations for charged redox species undergoing a redox process that leads to a charged product. In the case of electrophoretic migration of large colloidal particles, the effect of the increase in the strength of the electric field is masked by the blocking effect of the electrode insulation (glass), which limits the access of particles to the gap. One should keep in mind that at very low concentrations of particles (~femtomolar and less), the distance between them can be larger than the size of the tip electrode and the area of solution where the electric field is strong enough to pull the particles by migration. Therefore, glass insulation physically prevents particles from reaching by diffusion to the high electric field strength area between the tip and substrate electrodes, and the decrease in the rate of collisions is observed.

CONCLUSIONS

In this paper, we have presented the results of both experimental and theoretical investigations of electrophoretic migration of ions and charged particles in low electrolyte concentration media under the conditions of positive feedback SECM experiments. Theoretical data clearly shows an increase in the strength of the electric potential gradient in solution upon approach of the tip electrode to the substrate or counter electrode surface; this is commensurate with the increase in the flux of the redox species and the faradaic current at the tip due to the recycling of the species at the other electrode. However, the magnitude of the effect is not big at interelectrode gap sizes larger than the diameter of the tip electrode, because most of the potential drop in solution near the disk microelectrode occurs at a distance comparable to the electrode size. If the reactant of the tip reaction is a charged species, then the effect of migration is observed as the change in the magnitude of the tip current. However, once the current is normalized with respect to its value in the bulk solution, the normalized approach curve is identical to the approach curve obtained under the condition of purely diffusional mass transport of the depolarizer.

The effect of migration on the transport of charged nanoparticles in the gap was expected to be experimentally observable, because the magnitude of their charge is much bigger than that of the ions and the strength of the electric field increases upon closing of the electrode gap. However, the frequency of collisions of the insulating particles with the tip electrode surface has been shown to decrease as the size of the gap decreases (negative feedback). This observation is rationalized by the blocking effect of the glass insulation and relatively small volume of solution that is accessible to the electric field near the tip electrode compared to the interparticle distance (in solutions with very low concentration of the particles). Moreover, at small interelectrode gap sizes (comparable to the size of the tip), particle collisions with the tip electrode surface lead to observable changes in the faradaic current both at the tip and substrate electrodes. This finding serves as a direct confirmation of the high rate of mass transfer of the redox species in the gap between the electrodes under the conditions of positive feedback SECM experiments.

ASSOCIATED CONTENT

Supporting Information

Detailed descriptions of the numerical simulations used to describe migration effect in SECM. This material is available free of charge via the Internet at http://pubs.acs.org.

AUTHOR INFORMATION

Corresponding Author

*A. J. Bard. Phone: (512) 471-3761. Fax: (512) 471-0088. E-mail: ajbard@mail.utexas.edu.

Present Address

†The University of Akron, Department of Chemistry, Akron, OH 44325-3601

Author Contributions

The paper was written through contributions of all authors. All authors have given approval to the final version of the paper.

Notes

The authors declare no competing financial interest.

ACKNOWLEDGMENTS

This work was supported by the Department of Defense, Defense Threat Reduction Agency (Contract No. HDTRA1-11-1-0005).

REFERENCES

(1) Bard, A. J.; Mirkin, M. V. *Scanning Electrochemical Microscopy*, 2nd ed.; Taylor & Francis: Boca Raton, FL, 2012.

(2) Fan, F. R.; Bard, A. J. *Science* **1995**, *267* (5199), 871−874.

(3) Boika, A.; Thorgaard, S. N.; Bard, A. J. *J. Phys. Chem. B* **2013**, *117* (16), 4371−4380.

(4) Xiao, X.; Fan, F.-R. F.; Zhou, J.; Bard, A. J. *J. Am. Chem. Soc.* **2008**, *130*, 16669−16677.

(5) Zhou, H.; Fan, F.-R. F.; Bard, A. J. *J. Phys. Chem. Lett.* **2010**, *1*, 2671−2674.

(6) Tschulik, K.; Palgrave, R. G.; Batchelor-McAuley, C.; Compton, R. G. *Nanotechnology* **2013**, *24* (29), 295502.

(7) Stuart, E. J. E.; Rees, N. V.; Cullen, J. T.; Compton, R. G. *Nanoscale* **2013**, *5* (1), 174−177.

(8) Stuart, E. J. E.; Zhou, Y.-G.; Rees, N. V.; Compton, R. G. *RSC Adv.* **2012**, *2* (17), 6879−6884.

(9) Park, J. H.; Thorgaard, S. N.; Zhang, B.; Bard, A. J. *J. Am. Chem. Soc.* **2013**, *135* (14), 5258−5261.

(10) Cheng, W.; Zhou, X.-F.; Compton, R. G. *Angew. Chem.* **2013**, *125*, 1−4.

(11) Kim, B.-K.; Boika, A.; Kim, J.; Dick, J. E.; Bard, A. J. *J. Am. Chem. Soc.* **2014**, *136* (13), 4849−4852.

(12) Bard, A. J.; Zhou, H.; Kwon, S. J. *Isr. J. Chem.* **2010**, *50*, 267−276.

(13) Zhou, H.; Park, J. H.; Fan, F.-R. F.; Bard, A. J. *J. Am. Chem. Soc.* **2012**, *134* (32), 13212−13215.

(14) Sun, P.; Mirkin, M. V. *J. Am. Chem. Soc.* **2008**, *130* (26), 8241−8250.

(15) Kwon, S. J.; Bard, A. J. *J. Am. Chem. Soc.* **2012**, *134* (16), 7102−7108.